ORIGINAL ARTICLE

Identifying cellular signalling molecules in developmental disorders of the brain: Evidence from focal cortical dysplasia and tuberous sclerosis

Yao-Feng Li[1,2,3] | Fatma Scerif[1] | Simon R. Picker[1] | Thomas J. Stone[1,2] | Jessica C. Pickles[1,2] | Dale A. Moulding[4] | Aimee Avery[2] | Alex Virasami[1,2] | Amy R. Fairchild[1,2] | Martin Tisdall[5] | William Harkness[5] | J Helen Cross[6] | Darren Hargrave[1,7] | Francois Guillemot[8] | Simon M. Paine[9] | Shireena A. Yasin[1,2] | Thomas S. Jacques[1,2]

[1]Developmental Biology and Cancer Research & Teaching Department, UCL Great Ormond Street Institute of Child Health, London, UK

[2]Departments of Histopathology, Great Ormond Street Hospital NHS Foundation Trust, London, UK

[3]Pathology Department, Tri-Service General Hospital & National Defence Medical Centre, Taipei, Taiwan

[4]ICH GOS Imaging Facility, UCL Great Ormond Street Institute of Child Health, London, UK

[5]Neurosurgery, Great Ormond Street Hospital NHS Foundation Trust, London, UK

[6]Neurosciences Unit, UCL Great Ormond Street Institute of Child Health, London, UK

[7]Neuro-Oncology, Great Ormond Street Hospital NHS Foundation Trust, London, UK

[8]Neural Stem Cell Biology Laboratory, The Francis Crick Institute, London, UK

[9]Department of Neuropathology, Queens Medical Centre, Nottingham University NHS Trust, Nottingham, UK

Correspondence
Thomas S. Jacques, UCL Great Ormond Street Institute for Child Health, 30 Guilford Street, London WC1N 1EH, UK.
Email: t.jacques@ucl.ac.uk

Abstract

Aims: We understand little of the pathogenesis of developmental cortical lesions, because we understand little of the diversity of the cell types that contribute to the diseases or how those cells interact. We tested the hypothesis that cellular diversity and cell–cell interactions play an important role in these disorders by investigating the signalling molecules in the commonest cortical malformations that lead to childhood epilepsy, focal cortical dysplasia (FCD) and tuberous sclerosis (TS).

Methods: Transcriptional profiling clustered cases into molecularly distinct groups. Using gene expression data, we identified the secretory signalling molecules in FCD/TS and characterised the cell types expressing these molecules. We developed a functional model using organotypic cultures.

Results: We identified 113 up-regulated secretory molecules in FCDIIB/TS. The top 12 differentially expressed genes (DEGs) were validated by immunohistochemistry. This highlighted two molecules, Chitinase 3-like protein 1 (CHI3L1) and C-C motif chemokine ligand 2 (CCL2) (MCP1) that were expressed in a unique population of small cells in close proximity to balloon cells (BC). We then characterised these cells and developed a functional model in organotypic slice cultures. We found that the number of CHI3L1 and

CCL2 expressing cells decreased following inhibition of mTOR, the main aberrant signalling pathway in TS and FCD.

Conclusions: Our findings highlight previously uncharacterised small cell populations in FCD and TS which express specific signalling molecules. These findings indicate a new level of diversity and cellular interactions in cortical malformations and provide a generalisable approach to understanding cell–cell interactions and cellular heterogeneity in developmental neuropathology.

KEYWORDS

epilepsy, balloon cells, focal cortical dysplasia, tuberous sclerosis, CHI3L1, CCL2, molecular profiling, slice culture

INTRODUCTION

Epilepsy caused by focal cortical lesions in early childhood is a major cause of disability.[1] Our understanding of the cellular pathogenesis underlying these cortical lesions is limited because we understand little of the diversity of abnormal cell types within them, or how these different cell types interact to cause the disease.

Two of the most common developmental cortical lesions are focal malformations, focal cortical dysplasia (FCD) and cortical tubers in tuberous sclerosis (TS). FCD is the most common cortical lesion leading to multidrug-resistant epilepsy in children[2] and is characterised by disorganisation of the cortex and variable cytological abnormalities depending on the subtype. It is classified into three main types, FCD I, II and III. In particular, FCD type II is characterised by abnormally large pathological cells, dysmorphic neurons (DNs) in type IIA and IIB, and balloon cells (BCs) in type IIB.[3,4]

Patients with the genetic disorder tuberous sclerosis develop cortical lesions (tubers) that are histologically indistinguishable from the lesions seen in FCDIIB.[5] In both diseases, the lesions are thought to arise through activation of the mTOR pathway. In TS, this is due to germline mutations in either *TSC1* or *TSC2*[6] and in some patients with FCD, by somatic mutations in the mTOR pathway.[7-9]

Our understanding of the pathology of the lesions may be over-simplified as it lacks consideration of other cells that may contribute to disease pathogenesis. The full extent of the cell types implicated in FCD and their interactions within the lesional tissue is still currently unknown. For example recent studies have suggested an important role for inflammatory cells and inflammatory components as well as oxidative stress in the pathogenesis.[10] In particular, a recent study demonstrated strong staining for the inflammatory markers iNOS, xCT, TLR4 and COX-2 in BCs, DNs and smaller glial cells.[11] These markers have been shown to be involved in initiating inflammatory responses and to contribute to seizure development.[12]

We sought to identify potential interactions between pathological cells in FCDIIB and cortical tubers in an attempt to understand the cellular microenvironment that might lead to the pathology seen in these tissues. We hypothesised that cellular diversity and cell–cell interactions play an important role in these disorders and

characterised novel small cell populations in these lesions and determined whether the mTOR signalling pathway, known to be aberrant in FCD may affect them.

MATERIALS AND METHODS

Sample collection

Both fresh and formalin-fixed paraffin-embedded (FFPE) tissue were obtained from the histopathology department at Great Ormond Street Hospital. All samples were taken from excess surgical material and were reviewed by an experienced paediatric neuropathologist and classified according to the International League Against Epilepsy (ILAE) classification of FCD.[4] Normally formed cortex, lacking specific pathology, from patients undergoing temporal lobectomy for Hippocampal Sclerosis (HS) was used as control tissue. Ethical approval was granted (REC Approval # 05/Q0508/129).

RNA preparation and Affymetrix™ Human Exon 1.0ST microarray

Fifteen cases of different FCD subtypes (5 FCDIIB, 5 TS and 5 FCDIIA) were analysed. Another five samples of normal neocortex removed during surgery for HS were used as controls as they contained normally formed tissue that has previously been exposed to seizures. Fresh frozen samples from the selected cases were cut in half. One half was used for RNA extraction, and the other was used to generate frozen haematoxylin- and eosin-stained sections for pathological review and diagnostic confirmation. RNA was extracted using the Qiagen miRNeasy mini-kit. Eluted RNA was subjected to quality control by analysis on a NanoDrop 1000 spectrophotometer and samples with a 260/280 ratio lower than 1.8 were excluded. Further quality control was carried out using the Agilent Bioanalyzer platform and samples with an RNA Integrity Number (RIN) lower than four were excluded. The microarray was performed by UCL Genomics, using total RNA extracted from all 20 cases. RNA samples were processed on Affymetrix exon arrays

IDENTIFYING CELLULAR SIGNALLING MOLECULES IN DEVELOPMENTAL DISORDERS OF THE
BRAIN: EVIDENCE FROM FOCAL CORTICAL DYSPLASIA AND TUBEROUS SCLEROSIS

Neuropathology and
Applied Neurobiology—WILEY | 783
JOURNAL OF THE BRITISH NEUROPATHOLOGICAL SOCIETY

1.0 ST v2 arrays.[13] Raw microarray data (.CEL files) were normalised using the Robust Multi-array Average (RMA) algorithm. After normalisation, boxplots representing the distribution of intensities across each sample were used to check for appropriate normalisation and detect outliers.

Analysis of expression data

Hierarchical clustering analysis and heatmaps

Expression data from Affymetrix Human Exon 1.0 ST v2 arrays were read into R using the *oligo* package. Data were normalised using the RMA method as implemented in *oligo*. Annotation for the arrays was retrieved from the *huex10sttranscriptcluster.db* R package and Affymetrix transcript cluster IDs within the dataset were matched to their respective gene symbols for downstream analysis. A minority of gene symbols were duplicated, due to multiple exons from the same gene being represented on the array. In these instances, the duplicate entries were collapsed into one gene-level entry using the sum of the exon-level expression data. Subsequently, the median absolute deviation was used to determine the top 5000 most variable genes across the cohort. Unsupervised consensus clustering was then performed using the *ConsensusClusterPlus* R package using the WardD2 implementation of Ward's clustering method, a maximum K of 6 and 10,000 repetitions. After consensus clustering, the resulting groups were used for differential expression testing, performed using the *limma* R package and following the protocol described in the package vignette. Cases were divided into three groups based on consensus clustering (groups 1, 2 and 3). Differential expression comparisons were generated with a cut off of 0.05 for false discovery adjusted *p*-value was used to determine significance.

Gene set enrichment analysis (GSEA)

Gene set enrichment analysis of expression data was performed on the full expression dataset, using expression values after normalisation. Consensus clustering groups were used for comparisons. Data were analysed against the hallmark gene sets v7.1 available in the Molecular Signatures Database. For all other parameters, the default settings were used.

Ingenuity pathway analysis

To identify markers that could indicate active signalling between various cell types in the tissue, we uploaded the list of DEGs into Ingenuity Pathway Analysis (IPA) (http://www.ingenuity.com, Spring 2020 Release version). 1363 DEGs were uploaded into IPA. The following filters were applied when uploading and analysing the data: both indirect and direct relationships were considered. All data sources available were used. No other filters or restrictions were applied.

DAB Immunohistochemistry

DAB immunohistochemistry (IHC) was used to validate markers identified by IPA in tissue sections and organotypic brain slice cultures. Antibodies were selected based on online reviews in CiteAb (https://www.citeab.com/), and those used are listed in Supplementary material 1. Immunohistochemical staining was performed using a Leica Bond—Max[TM] autostainer (Leica Microsystems) with appropriate positive and negative controls. Antigen retrieval methods were optimised for each antibody.

Scoring of IHC staining

For evaluating the IHC staining, the whole tissue area (containing grey and white matter) was used for analysis. The staining of extracellular markers was semi-quantitatively assessed and the intensity of staining was scored as follows for each cell type (0 = negative, 1 = weakly positive, 2 = moderately positive, 3 = strongly positive). The mean score for each stain was calculated across different cell types and brain structures (BCs, DNs, normal neurons, small glial cells, endothelial cells, neuropil and white matter). For organotypic slice cultures, IHC staining was automated and images were then evaluated. Slides were digitalised and exported as 10× tiff figures. The entire area was then automated and quantified using Fiji software and the particle or area quantification macro was used depending on the cellular localisation of the marker. Radar plots were used to compare the IHC scores between BC and control groups.

Immunofluorescence (IF)

FFPE slides were dewaxed in xylene and rehydrated through a graded alcohol series. Antigen retrieval was performed in a pressure-cooker at 125°C in EDTA-Citrate buffer pH 6.2. 10% hydrogen peroxidase was used to block endogenous peroxidase activity. Sections were blocked in 40% heat-inactivated sheep serum diluted in PBS with 0.2% bovine serum albumin, 0.15% glycine, 0.1% Triton X-100 at room temperature for 1 h. Sections were then incubated with primary antibodies at 4°C overnight in a sealed and humid chamber. The following morning, sections were rinsed with dH$_2$O and washed twice in 0.1% Tween/PBS for 3 min and then incubated with Alexa Fluor 488, 568 or 647 secondary antibodies (Life Technologies) for 1 h. After incubation, slides were washed and treated with 0.1% Sudan Black for 20 min to reduce tissue autofluorescence.[14] Finally, slides were washed three times in PBS for 3 min and mounted in Vectashield aqueous mounting medium containing 4', 6-diamidino-2-phenylindole/DAPI (Vector) before imaging.

Slice culture treatment with the mTOR inhibitor (Everolimus)

Six surgical samples from three patient cases (1 sample from 1 FCDIIB case and 5 independent samples from 2 TS cases) were used to prepare slice cultures using the technique by Stoppini *et al.*[15] Briefly, fresh samples were cut into 400-μm-thick sections using a tissue chopper (Nickle Laboratory Engineering Co. Surrey). The standard thickness of organotypic brain slice cultures in the literature ranges from 100 to 400 μm.[16,17] We found that in our hands that 400 μm was the optimal thickness to maintain tissue integrity while allowing a detailed three-dimensional analysis of the cell types and interactions between them in the tissue. This is in keeping with many other studies that have also found this tissue thickness to be optimal for slice cultures.[18-24]

For optimisation experiments (supplementary_6), six individual samples derived from six patients were collected. Each sample was then sectioned for the control and experimental group and compared weekly (Day0 x 1, Day1, Day7, Day14, Day21, Day28). Hence, 11 slices were sectioned from each sample. Therefore, 66 organotypic slice cultures were assayed. Additionally, in the mTOR experiments (Figure 6), another six samples were derived from three patients, including one FCDIIB and two TS cases. Similarly, each piece was sectioned into two slices for the experimental and control experiments. Therefore, a total of 12 slice cultures were assessed here.

Slices were cultured in 1.5 ml defined media (DMEM/F12 (Sigma) supplemented with B27 supplement (Invitrogen), 100 units/ml penicillin, 0.1 mg/ml streptomycin (Sigma), 20 ng/ml FGF2, 20 ng/ml EGF (Peprotech), or with 10% FBS, 2% N2 and 20 ng/ml NGF (Sigma) in inserts (0.4 μm Millicell-CM culture plate insert; Millipore) in six-well plates, and incubated at 37°C with 5% CO_2 for 2 days. Following the optimisation of the culture medium, slices were separated into three groups of different treatment conditions, defined media containing 0.02% DMSO, 1 μM Everolimus and 5 μM Everolimus respectively. The culture media was changed daily. Five days of post-treatment, slices were fixed in 10% non-buffered formalin before being processed for paraffin embedding.

Image J and statistics

ImageJ (https://fiji.sc/) was used to semi-quantify the level of CHI3L1, CCL2, pS6 and C-Caspase 3 staining. Slides were scanned using an Aperio CS2 slide scanner and exported at 10× magnification for further analysis. Statistical analysis of the slice culture staining was performed with SPSS version 22 using the Kruskall–Wallis test.

Passive clarity

The CLARITY technique was adapted from Deisseroth[25] and Gentleman *et al.*[26] Three cortical tubers from epilepsy surgery were sliced at a thickness of 400 μm and put into a hydrogel monomer comprised of 4% paraformaldehyde (PFA), 0.05% bis-acrylamide (Bio-Rad), 4% (vol/vol) acrylamide (Bio-Rad) and 0.25% VA-044 photo-initiator (Wako) in PBS for 7 days. Tissue slices were transferred into a 6 ml container followed by a layer of olive oil to prevent oxygen interference during hydrogel polymerisation and incubated at 37°C for 3 h. After removing excess hydrogel, tissue was passively cleared in clearing solution (4% SDS in 200 mM boric acid solution, pH8.5). The clearing solution was replaced every 3 days and samples were incubated at 50°C until transparent.

Post clearing, samples were washed with 0.2% PBST (PBS and 0.2% Triton-X) to remove residual SDS micelles, they were then blocked in a solution of 10% normal goat serum, 0.2% Triton-X and 0.05% sodium azide in PBS, shaking at 4°C for 3 days. Samples were incubated with 4 ml antibody diluent (1% normal goat serum, 0.2% Triton-X and 0.05% sodium azide in PBS) with 1:100 primary antibody at 4°C for 3 days; then washed in 0.2% PBST (3 × 12 h at 37°C) and incubated in 4 ml antibody diluent with 1:100 secondary antibody at 4°C for another 3 days. They were then incubated in 4′, 6-diamidino-2-phenylindole (DAPI) at 1 μg/ml to label all cell nuclei and were washed in 0.2% PBST (3 × 12 h at 4°C) and transferred to new 15 ml centrifuge tubes containing 30% 2,2-Thiodiethanol (TDE) (Sigma) in 1× PBS for 24 h, and then 63% TDE for another 24 h. Stained slices were mounted in chamber slides containing 63% TDE in 1× PBS for image analysis.

Confocal microscopy 3D image construction

Fluorescent slides/samples were imaged using a Zeiss Examiner LSM 880 confocal microscope driven by ZEN imaging software (Zen2.3; Zeiss) and equipped with a 20×/NA1.0 Plan Apochromat Water objective correction collar. Fluorophore excitation and scanning were performed with laser excitation at 405, 488, 561 and 633 nm. The pinhole was set equivalent to 1 AU. Image size *x*, *y*, *z* was 136.58 × 136.58 × 75.98 μm, the XY resolution was set to 0.42 μm and the bit depth was set to 8. The *z*-width and resolution were 75.98 and 0.58 μm, respectively, per slide.

To examine the three-dimensional morphology of cell types in FCDIIB/TS, we used the image analysis software Imaris 8.0. Briefly, confocal images were loaded into the software. The surface grain size was set at 2 μm. The threshold was then set for the fluorescent signal and the artificial surface was set according to the original level of immunofluorescence. As mentioned in the section scoring of IHC staining above, Fiji software was used for automated signal quantification based on the staining pattern. Markers such as CCL2, CHI3L1 and Cleaved Caspase-3, were quantified using the Fiji particle macro. The staining intensity thresholds were 0–90 and the particle size range was 15–500 $μm^2$. For staining heavily expressed in cell processes, such as for pS6, the area was quantified using the Fiji area macro.

IDENTIFYING CELLULAR SIGNALLING MOLECULES IN DEVELOPMENTAL DISORDERS OF THE
BRAIN: EVIDENCE FROM FOCAL CORTICAL DYSPLASIA AND TUBEROUS SCLEROSIS

Neuropathology and
Applied Neurobiology—WILEY 785

RESULTS

Unsupervised clustering of transcriptional profiles of malformations

In order to determine the signalling molecules expressed in different cell populations in this spectrum of malformations, we undertook transcriptional analysis of cases FCDIIB (by definition containing balloon cells), TS cases (which resemble FCDIIB, and in particular contain balloon cells), FCDIIA (mimicking all the cytological components of FCDIIB except for balloon cells) and normally formed cortex from patients with epilepsy (HS cases). We assessed adjacent frozen sections to ensure that the histological features were representative of each disease. Nonetheless, as this is adjacent tissue from diseases that show variable cellular content in different regions, we predicted that the numbers of each cell type would vary in each sample (e.g. BCs or DNs may have been under-represented in some samples). Therefore, we undertook unsupervised clustering of the transcriptional profiles to identify the underlying biological groups, in a way that was not dependent on the variability of the cellular components in any individual sample (Figure 1A).

To determine the optimal number of groups that explained the variability in the data, we used the CDF plot (Figure 1B). This revealed that cases clustered best into three molecularly defined groups and that a fourth group would not explain significantly more variability in the data. We analysed the differentially expressed genes between each of the three groups and these data are given in supplementary material 2.

There was a correlation between the underlying histopathology and the molecularly defined groups, for example the first group was a pure balloon cell group and consisted of four FCDIIB and three TS (group 1, $n = 7$), the second consisted of one FCDIIB, two TS, three FCDIIA and one HS case (group 2, $n = 7$), the third group consisted of two FCDIIA and four HS cases (group 3, $n = 6$) (Figure 1A). However, as we predicted, this was not an absolute relationship between molecularly defined groups and histologically defined groups, possibly due to variability in sampling different types of cells in each sample. We focussed on the molecularly defined groups to define expression patterns and in particular, focussed on differential gene expression between the pure BC and non-BC groups, that is group 1 and group 3.

Differentially expressed genes and pathways

A total of 1363 Differentially Expressed Genes (DEGs) were identified by comparing group 1 and group 3, including 847 up-regulated and 516 down-regulated DEGs (Supplementary material 2). IPA analysis of the DEGs showed that the top altered canonical pathways were inflammatory, signalling through the Rho Family GTPases, Leucocyte Extravasation Signalling, IL-8 Signalling and finally the Endocannabinoid Neuronal Synapse Pathway (Supplementary material 3). The key altered molecular and cellular functions determined

by IPA were cell movement, cell–cell signalling and interactions, cellular compromise, cell death and survival, cellular assembly and organisation.

Gene set enrichment analysis (GSEA) of the DEGs showed 43 gene sets up-regulated in group 1. The 36 gene sets were significant at a false discovery rate (FDR) of <25%, including 24 gene sets, which were significantly enriched at the nominal p-value <5%. Many enriched gene sets were associated with neuroinflammation, including IL6_JAK_STAT3_SIGNALING, COMPLEMENT, INTERFERON _GAMMA_RESPONSE, TGF_BETA_SIGNALING, IL2_STAT5_ SIGNALING, TNFA_SIGNALING_VIA_NFKB, INFLAMMATORY_ RESPONSE and INTERFERON_ALPHA_RESPONSE pathways (Supplementary material 2 and 4) These results support the IPA analysis, which highlights the role of neuroinflammation in group 1 versus group 3. Furthermore, in the GSEA analysis, PI3K_AKT_ MTOR_SIGNALING was also identified, but only revealed borderline significant ($p = 0.052$).

### Immunohistochemical analysis of differentially expressed genes

In order to understand cell–cell signalling in FCD, we focussed on DEGs that encoded for proteins located in the extracellular space. In total, there were 133 DEGs encoding for extracellular molecules, of which 113 were up-regulated and 20, down-regulated in group 1. We focussed on the top up-regulated DEGs and validated 12 of them (SERPINA3, Ceruloplasmin(CP), LUM, CCL2, HGF, TNC, CHI3L1, EFEMP1, ECM2, ANGPT1, SERPING1 and MANT2; Figure 1C,D) by immunohistochemistry (IHC). As the histology consists of a complex mixture of cell types, we assessed patterns of expression by cell type. All these DEGs showed different patterns of expression between FCD cases and control normally formed cortex (Figure 1D), providing validation of the transcriptional data.

Of note, while all markers showed different patterns of expression between, two markers, CHI3L1 and CCL2, were distinguished by predominant expression in populations of small cells seen in BC-cases (i.e. FCDIIB and TS) that were not seen in controls (HS). We, therefore, sought to characterise the cells secreting CHI3L1 and CCL2.

Strong cytoplasmic CHI3L1 staining was seen in a subpopulation of cells which morphologically resembled small glial cells (Figure 2) (mean cell body length = 13.67 μm (±0.25 μm SEM, $n = 3$)). In contrast, most BCs were negative for CHI3L1, but a few had weak cytoplasmic staining (compared to the small cell population) ($n = 10$, 5 BC group cases and 5 non-BC group cases). Neurons in both the BC and non-BC cases were negative, and there was no staining for CHI3L1 in FCDIIA cases or in normally formed neocortex from HS cases, indicating that CH13L1 expression in small glial cells was present only in cases with BCs. To explore the potential for a direct interaction between BCs and CHI3L1-positive cells, immunostaining for the CHI3L1 receptor, IL-13Rα2 was performed on three FCDIIB and two TS cases. All BCs were found to express IL-13Rα2 (Supplementary material 5).
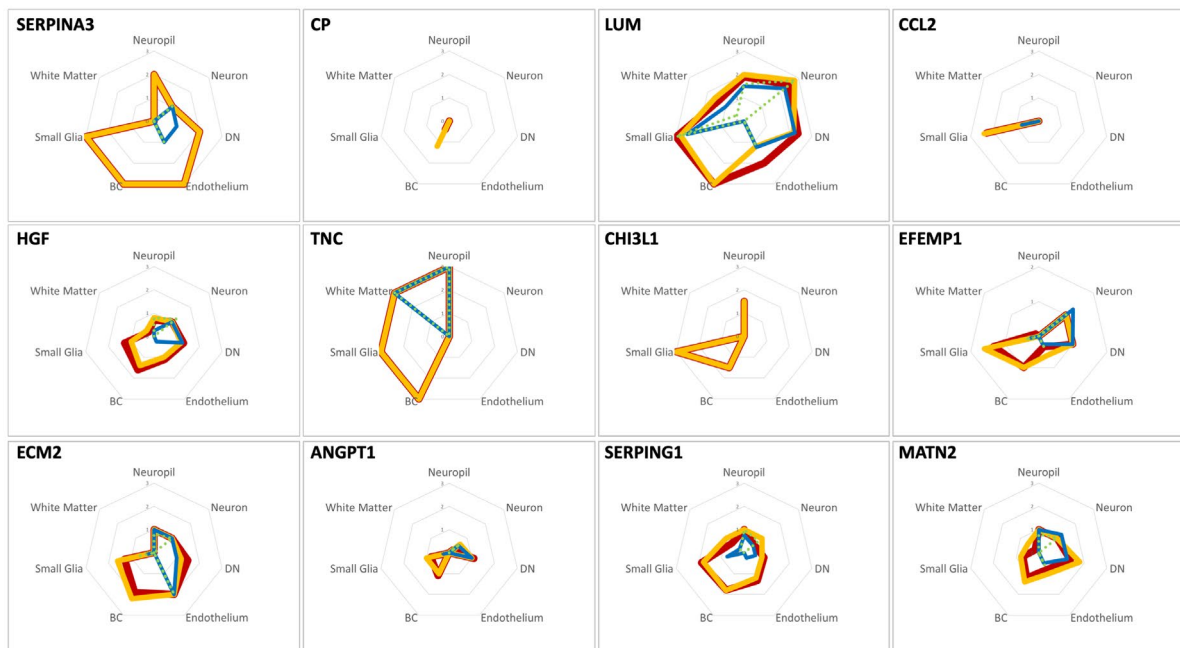
By double labelling, a proportion of CHI3L1-positive cells (57.1%) expressed GFAP, an astrocytic and progenitor cell marker (Figure 3).[27] Most CHI3L1-positive cells expressed the stem and progenitor cell marker, SOX2 (91.6%), some expressed Nestin (35.6%), Vimentin (12.1%) or Reelin (19.6%). 99.1% of CHI3L1-positive cells were immunoreactive for S100β and most expressed GFAP-δ (83.6%), two glial progenitor cell markers.[28,29] In contrast, CHI3L1-positive cells were negative for neuronal markers (DCX, TuJ-1 and NeuN) and microglial markers (CD68 and Iba-1). These data suggest that CHI3L1-positive cells are, by phenotypic criteria, most likely to be glial progenitors.


(A)

(B) Delta area
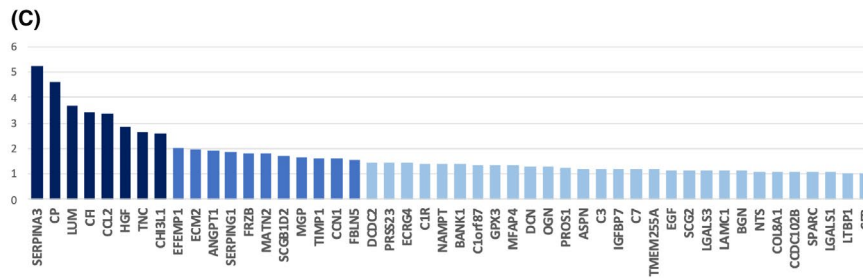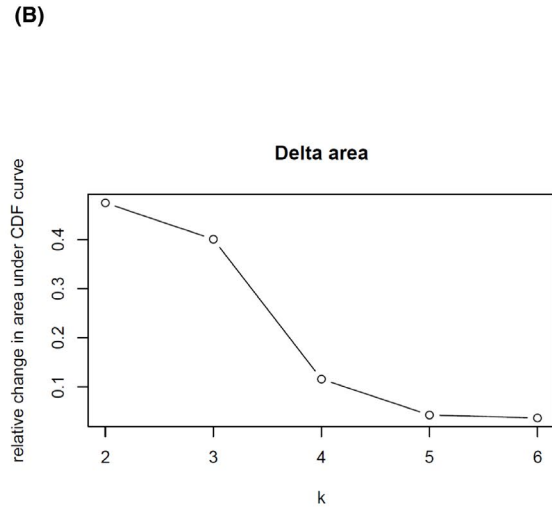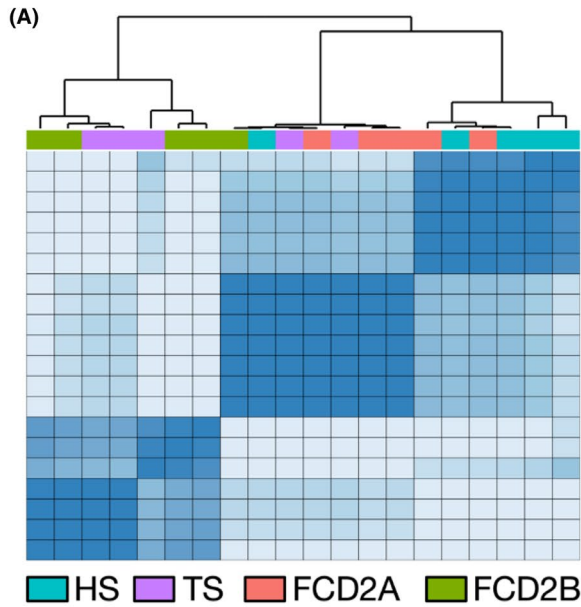
Gene Symbol	logFC	P.Value	adj.P.Val
SERPINA3	5.212	3.71E-08	3.67E-05
CP	4.637	1.00E-06	2.77E-04
LUM	3.682	9.33E-06	1.05E-03
CCL2	3.370	4.01E-06	5.96E-04
HGF	2.850	6.07E-08	5.29E-05
TNC	2.653	6.05E-07	2.08E-04
CHI3L1	2.613	1.01E-03	1.90E-02
EFEMP1	2.025	3.86E-04	1.04E-02
ECM2	1.984	3.21E-09	1.19E-05
ANGPT1	1.892	1.80E-04	6.62E-03
SERPING1	1.890	6.76E-07	2.19E-04
MATN2	1.796	4.19E-06	6.03E-04

IDENTIFYING CELLULAR SIGNALLING MOLECULES IN DEVELOPMENTAL DISORDERS OF THE
BRAIN: EVIDENCE FROM FOCAL CORTICAL DYSPLASIA AND TUBEROUS SCLEROSIS

Neuropathology and
Applied Neurobiology—WILEY— 787
JOURNAL OF THE BRITISH NEUROPATHOLOGICAL SOCIETY

FIGURE 1 (A) Gene expression analysis clustered the four histological entities into three molecularly distinct groups. The figure shows a heatmap of the 20 cortical samples clustered into three groups and correlated with their histopathological type. (B) The area under the CDF plot showed only a small change at $K = 4$, suggesting that a three-cluster model was the optimal grouping to explain the variability in the data. (C) Expression levels of extracellular molecules up-regulated in group 1 compared to group 3. The colours of the bars represent increased log fold change (dark blue >2.5, royal blue 2.5–1.5 and light blue below 1.5-fold change). The table shows a summary of the top extracellular molecules up-regulated in group 1 compared to group 3. The molecules are listed by their decreasing log fold change (LogFC), which is shown alongside the p-value and adjusted p-value. (D) The top 12 up-regulated genes were selected for further validation by immunohistochemistry in examples of FCDIIB ($n = 10$, shown in red), FCDIIA ($n = 4$, shown in blue), TS ($n = 10$, shown in yellow) and normally formed cortex from HS cases ($n = 5$, shown in green). As the staining patterns are different in different cells types the expression was scored in each morphological defined cell types (BC (Balloon cells), DN (dysmorphic neurons), neurons (non-dysmorphic neurons), small glia and endothelial cells) and in the stroma of the neuropil and white matter. The staining was scored semi-quantitatively (on a scale of 0 to 3). The data are summarised in the radar plots such that increased staining score is represented as increased distance from the centre of the plot.
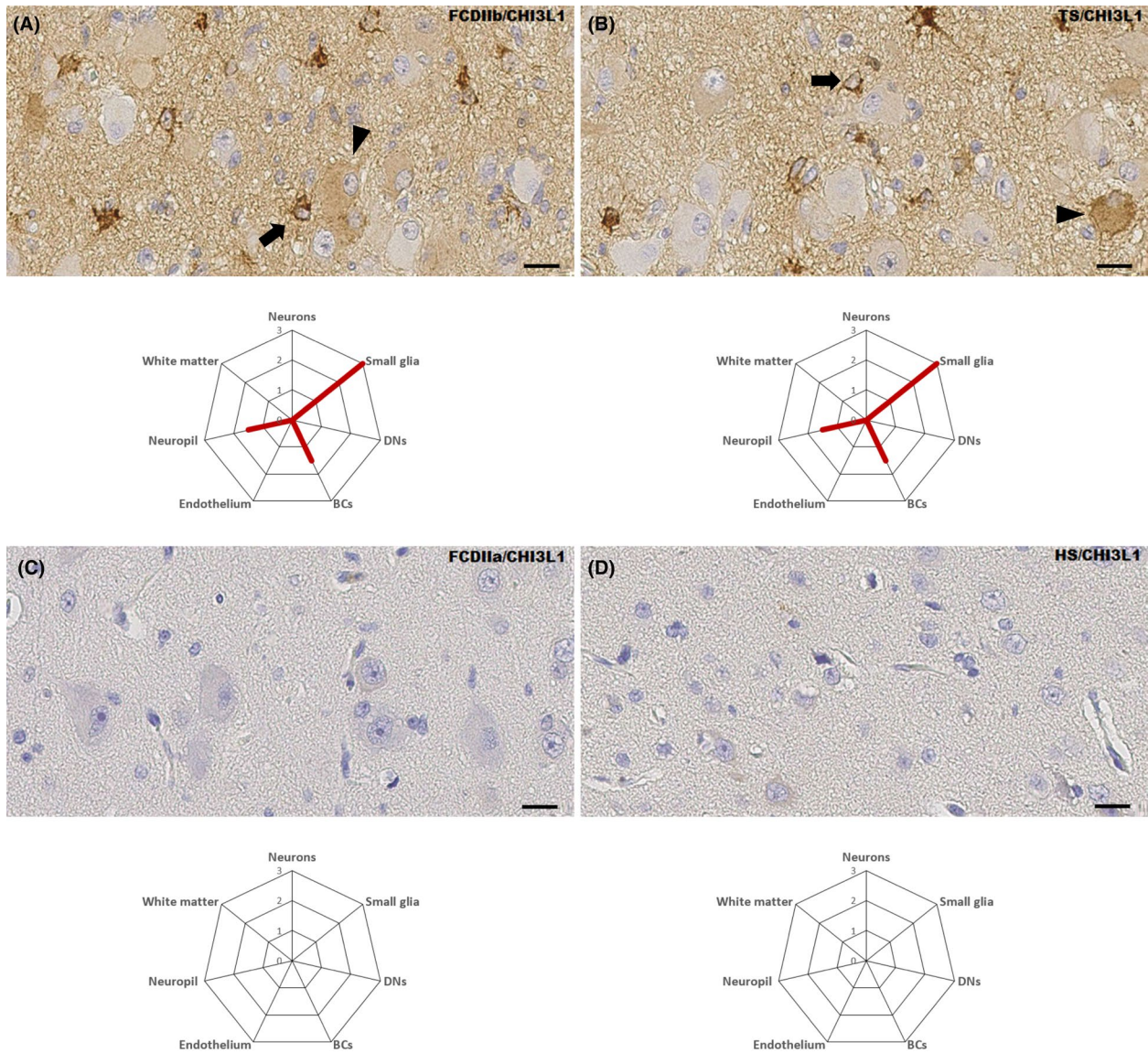
FIGURE 2 Chitinase 3 Like 1 (CHI3L1) immunostaining showing representative images of cases of FCDIIB (A) TS (B), FCDIIA (C) and normally formed cortex form HS cases (D). Arrows indicate the CHI3L1-positive cells, and the arrowheads show balloon cells. Scale bar 20 μm. The radar plots below show the semi-quantitative analysis of CHI3L1 expressing cells in the different cell types of cells in each tissue.
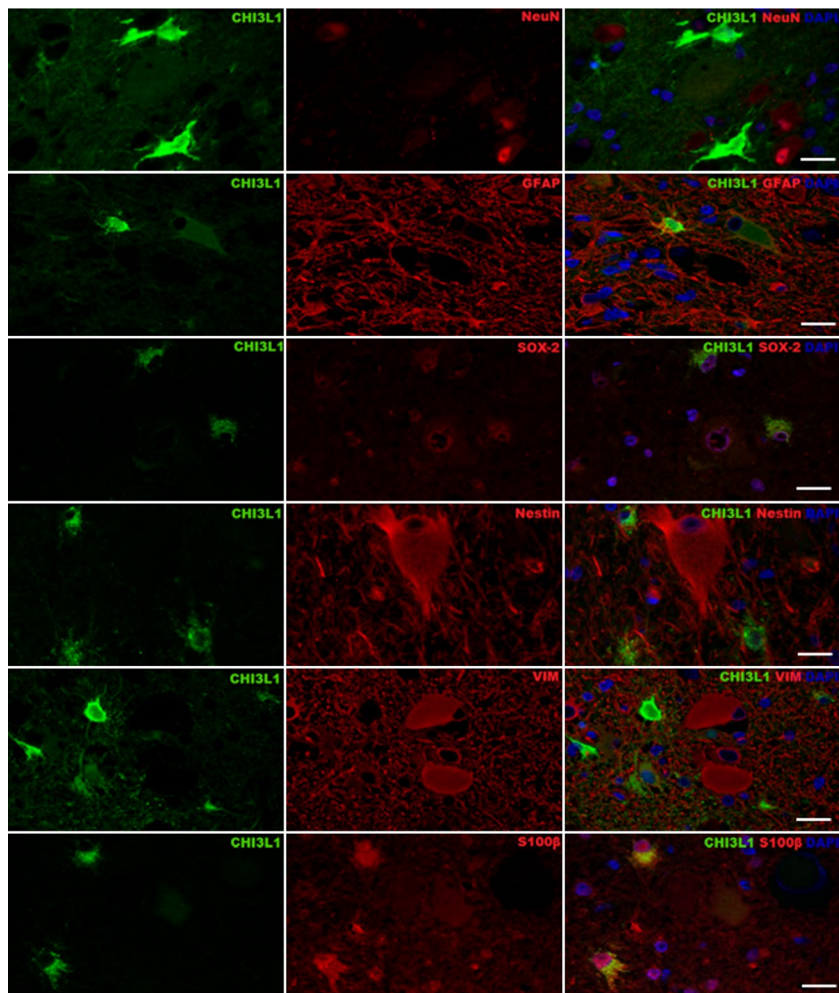
FIGURE 3 CHI3L1 expression in FCDIIB/TS cases. Co-localisation of CHI3L1 with cell lineages markers. CHI3L1 (green) co-stained with NeuN, GFAP, Sox2, Nestin, Vimentin and S100b (red). Blue = DAPI. The CHI3L1-positive cells have a phenotype most suggestive of glial progenitors. Scale bar 20 μm.

Characterisation of the CCL2-positive cells

Immunohistochemistry of FCD cases for CCL2 highlighted a population of small cells which resembled glial cells (Figure 4) (Mean cell body length was 11.98 μm (±0.19 μm, SEM, $n = 3$)). This population was present in all balloon cell cases tested (FCDIIB $n = 10/10$, and TS $n = 5/5$), some FCDIIA cases (FCDIIA $n = 2/4$) but was absent in the control neocortex (control $n = 0/5$).

90% of the CCL2-positive population co-localised with microglial markers, including CD68 (90%), Iba-1 (86%) and HLA-DR (88%) (Figure 5). 10.4% of CCL2-positive cells showed GFAP expression ($n = 3$ [2 FCDIIB and 1 TS]). There was no co-localisation with the neuronal markers, TUJ-1 or Neurofilament. These results suggest that most CCL2-positive cells belong to a microglial lineage. Indeed, we noted that there were occasional clusters of CCL2-positive cells, mimicking microglial nodules in tissue sections (data not shown).

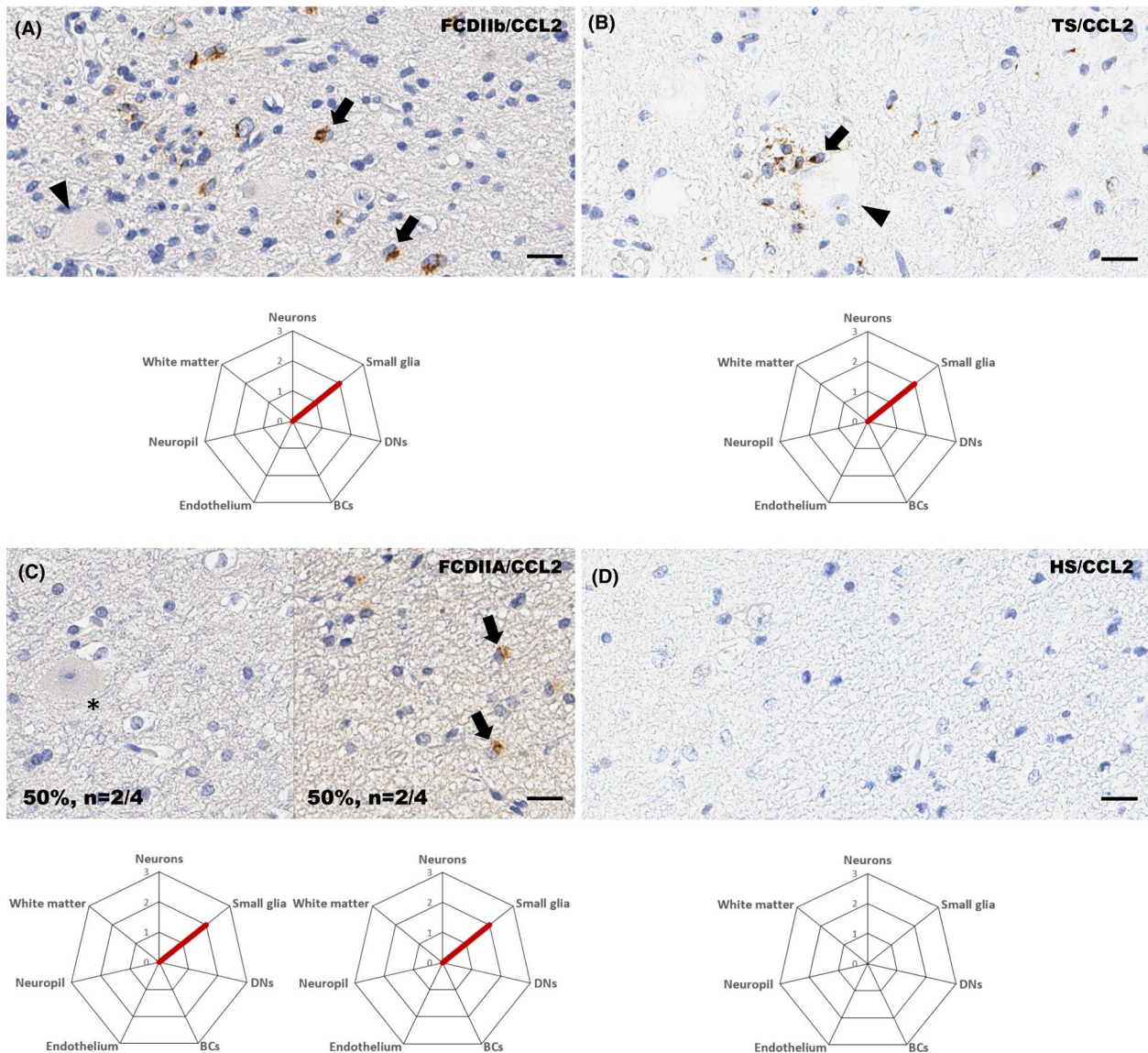## CHI3L1-positive and CCL2-positive cells are distinct populations

Based on size and phenotype, CH13L1- and CCL2-positive cells appeared to be different cell populations. To test this hypothesis, we performed double immunofluorescence staining on three different cases (2 FCDIIB and 1 TS). There was no co-localisation of CHI3L1 and CCL2 in any cells (Figure 6). To visualise the distribution and morphology of these different cell populations, we used the clearing technique CLARITY. Three-dimensional imaging of the samples showed that CHI3L1 and CCL2, were distinct cell populations found close to balloon cells (Figure 6 and Supplementary material 8), suggesting that there may be a complex local cellular microenvironment of signalling between these small and large cells in the lesional tissue.

Examining tissue architecture and cell types with organotypic slice cultures

In order to determine the functional relationship between these cells in FCDIIB and TS lesions, we used organotypic cultures. Slice cultures were optimised using non-lesional tissue according to established protocols.[15] We found optimal cell preservation with medium contained a combination of growth factors defined media (DMEM/F12 supplemented with B27, EGF and FGF) (Supplementary material 6). In control tissue, we saw the preservation of the major cell population and moreover, in FCDIIB and TS cases, we found the principal

IDENTIFYING CELLULAR SIGNALLING MOLECULES IN DEVELOPMENTAL DISORDERS OF THE
BRAIN: EVIDENCE FROM FOCAL CORTICAL DYSPLASIA AND TUBEROUS SCLEROSIS

Neuropathology and
Applied Neurobiology—WILEY | 789
JOURNAL OF THE BRITISH NEUROPATHOLOGICAL SOCIETY

FIGURE 4 CCL2 immunostaining showing representative images of cases of FCDIIB (A) TS (B), FCDIIA (C) and normally formed cortex form HS cases (D). Arrow indicates the CCL2-positive cells, and arrowhead shows balloon cells. Asterisks show dysplastic neurons. Scale bar 20 μm. The radar plots below the semi-quantitative analysis of CCL2 expressing cells in the different cell types of cells in each tissue.

pathological cell types were also maintained in the cultures over this time period, including Balloon cells, CCL2-positive and CHI3L1-positive cells (Supplementary material 7), therefore allowing us to investigate these cell types in an *in vitro* culture model.

mTOR inhibition leads to a reduction in CCL2- and CHI3L1-positive cells

mTOR hyperactivation is the driver in both FCDIIB and TS. If the CCL2- and CH13L1-positive cells are part of the cellular phenotype of the disease, we might predict that they would be under the control of this pathway. Therefore, we treated the slice cultures with the mTOR inhibitor, Everolimus. Following treatment of the slices with

Everolimus, the number of CHI3L1 and CCL2 expressing cells was significantly reduced ($p = 0.01$ and $p = 0.005$ respectively) (Figure 7). Phosphorylated S6 protein (pS6) an mTOR target, was also down-regulated in cells ($p = 0.006$), confirming that mTOR was effectively inhibited.

To determine whether the loss of cells was due to non-specific pharmacological toxicity, we evaluated the cleaved caspase-3 status in both the experimental and control groups. Both Everolimus-treated groups had lower levels of apoptotic cells (35.1 cells/mm^2 and 38.7 cells/mm^2 respectively) compared to the control group (175.8 cells/mm^2), $p = 0.013$ (Figure 7). This result confirms that there is no overall increase in apoptosis, suggesting that non-specific toxicity cannot account for the loss of CHI3L1 and CCL2 expressing cells in mTOR-inhibited FCD lesions.
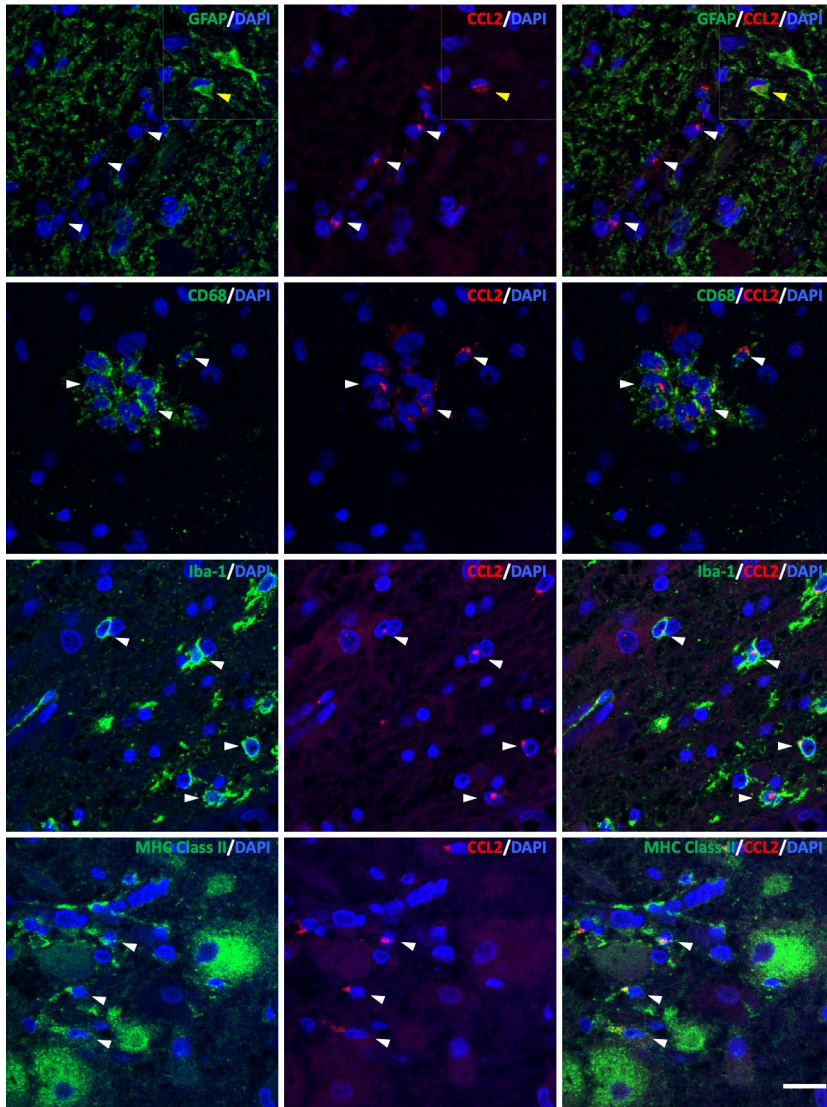
FIGURE 5 Double immuno-labelling shows that CCL2 expression colocalised with microglial markers (Iba-1, MHC Class II, CD68) and a few with the astrocytic marker, GFAP. There was no colocalisation identified with neuronal markers, Neurofilament and TUJ-1. White arrowhead indicates CCL2 (+) cells, yellow arrowhead shows colocalisation with GFAP. Scale bar is 20 μm.

DISCUSSION

In this study, we explored the cellular diversity and cell–cell interactions playing a role in the pathology of developmental cortical lesions, specifically FCD and TS lesions. Using unsupervised transcriptional profiling, we clustered cases into molecularly defined groups and compared the differential gene expression between the most histologically diverse of these groups. Using these differentially expressed genes we identified extracellular signalling molecules and showed that the top 12 all showed differential expression in dysplastic compared to normal cortex when assessed by immunohistochemistry. In particular, we focussed on two secreted molecules, CHI3L1 and CCL2, that were expressed uniquely in small glial cells (glial progenitors and microglial respectively) only in dysplastic cortex and showed that they are under the control of the mTOR pathway. This suggests that there is a heterogeneous population of cells, regulated by mTOR signalling, and that there is a complex network of signalling underlying the abnormalities in dysplastic cortex.

We took an unbiased clustering approach to segregate cases as this allowed us to control for variability in the cellular composition

of the samples. Moreover, it means we did not assume that the histologically defined subgroups represent uniform biological entities. Through this analysis, we focussed on secretory molecules that were differently expressed between different groups as this is likely to reveal both cellular heterogeneity and networks of cell to cell signalling. While many molecules showed disease-specific differential expression (both by RNA expression and immunohistochemistry), the two that we focussed on, CCL2 and CHI3L1, were found to be expressed only in populations of small glial cells unique to dysplastic cortex. These cells were not found in normally formed cortex from patients with epilepsy. The identification of a small cell component, particularly in close proximity to BCs and to each other raises the possibility of a complex microenvironment with the dysplastic cortex (Figure 8).

Based on their morphology and previous literature,[30] we hypothesised that the CHI3L1-positive cells in FCD were most likely to be microglia or astrocytes. To test this hypothesis, a lineage-based immunofluorescence approach was undertaken, which showed that CHI3L1 expression did not co-localise with neuronal (DCX, TuJ-1

IDENTIFYING CELLULAR SIGNALLING MOLECULES IN DEVELOPMENTAL DISORDERS OF THE
BRAIN: EVIDENCE FROM FOCAL CORTICAL DYSPLASIA AND TUBEROUS SCLEROSIS

Neuropathology and
Applied Neurobiology—WILEY | 791
JOURNAL OF THE BRITISH NEUROPATHOLOGICAL SOCIETY

FIGURE 6 The image shows the cellular microenvironment in BC dysplasia. (A–C) There is no colocalisation between CHI3L1 and CCL2 expression (demonstration of staining in case of TS). Scale bar 10 μm. (D) In order to visualise the microenvironment in three dimensions, Imiris software was used to infer the surface of cells within tissue from images obtained of CLARITY-processed tissue labelled with CHI3L1 (red), CCL2 cells (green) and vimentin giant cells (grey). See also supplementary material 8. Scale bar 50 μm.
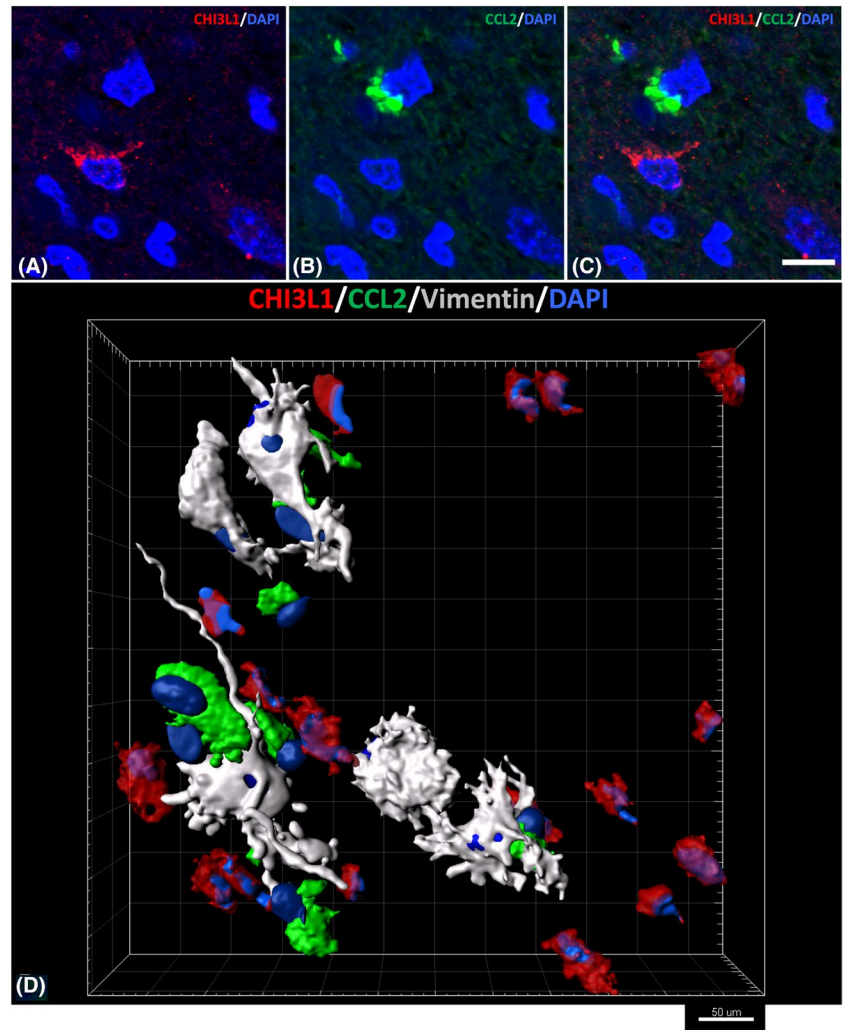

and NeuN) or microglial markers (CD68 and Iba-1) but did with glial and progenitor cell markers, suggesting the cells may be of glial progenitors.

In the central nervous system, up-regulation of CHI3L1 has been seen in many diseases, including encephalitis,[30] prion disease,[31] Alzheimer's disease,[32] amyotrophic lateral sclerosis,[33] multiple sclerosis,[34] trauma,[35] developmental status[36] and in glioblastoma.[37] The role of CHI3L1 in the central nervous system is unclear, but it has been suggested to be involved in tissue remodelling during inflammation,[38] to regulate excess inflammatory cell recruitment[35,39] and to promote cell survival.[40] Taken together with our data, this suggests that the CHI3L1-positive cells may either be part of an inflammatory response specific to FCDIIB/TS or may represent a developmentally abnormal cell population (in keeping with their progenitor cell phenotype).

We also found increased CCL2 expression in group 1. Double labelling studies showed that the majority of CCL2-positive cells co-localised with microglial markers (including CD68, Iba-1 and MHC class II) and a minority with astrocytic markers (GFAP). The cells were mostly found in FCDIIB/TS cases, and some were found in a few FCDIIA cases but were not present in the

normally formed cortex of patients with epilepsy. CCL2 has been previously described to be expressed not only in microglia but also in astrocytic cells and dysmorphic neurons.[41,42] A study by Diede *et al.* showed that CCL2 expression amongst other markers was related to the duration of seizures in rats and suggest that there is generally increased expression of CCL2 in the human epileptogenic hippocampus.[43] However, we did not see significant expression in the cortex of patients with HS, suggesting that the expression in FCD is not a non-specific reaction to seizures.

Recently, a growing body of evidence has shown increased neuroinflammation in FCDIIB and TS.[41,42,44,45,46] The release of proinflammatory mediators (such as complement, cytokines, chemokines) not only triggers the immune system but also act as neuromodulators, which direct excitability and induced epilepsy.[47-51] The increase of the classical complement system components was reported in the TS a few years ago.[41] Several pieces of research also suggest that C1q and C3 might play a role in mediating the elimination of CNS synapses.[52-55] Moreover, the activation of both innate and adaptive immune responses in FCDII was also noticed.[42,44,56] Our data also indicate an up-regulation of markers involved in neuroinflammation
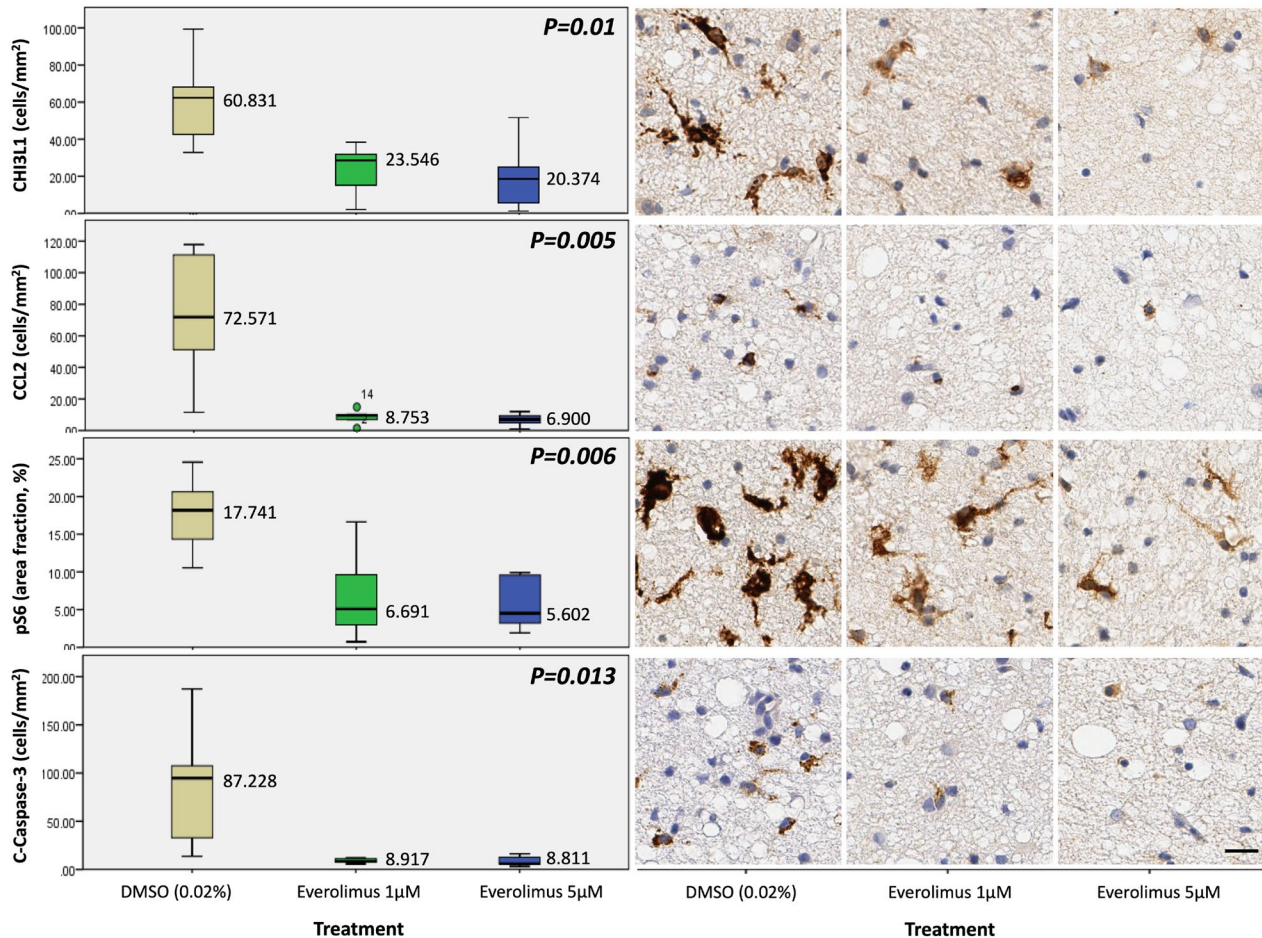
FIGURE 7 Following mTOR inhibitor treatment with Everolimus, the downstream marker of mTOR activation, pS6, was down-regulated ($p = 0.006$, Kruskall–Wallis test) compared to the control group. Quantification of CHI3L1 staining showed that mTOR inhibition decreased the CHI3L1-positive populations compared to the control group ($p = 0.01$, Kruskall–Wallis test). Similarly, mTOR inhibition reduced the CCL2 (+) population compared to controls ($p = 0.005$, Kruskall–Wallis test). Quantification of Cleaved Caspase-3 staining showed that mTOR inhibition did not result in more Cleaved Caspase-3 positive (apoptotic) cells compared to the DMSO control group ($p = 0.013$, Kruskall–Wallis test).

similar to previous studies, such as IL-1beta,[42] MCP1,[41,42] ECM2,[41] ANGPT1,[41] SERPINA3,[41] CHI3L2,[41,44] CP,[10,41] phospholipase A2 group IIA (PLA2G2A)[44] and C-C motif chemokine ligand 4 (CCL4).[44] Therefore, this inflammatory response may be an important mechanism which contributes to the pathogenesis and epileptogenesis in FCD lesions.

The global pathway centred approach, as opposed to investigating single gene / molecular alterations may be more useful in explaining local signalling and complex cell–cell interactions in developmental lesions. For example in a recent study, Kobow and colleagues used DNA methylation profiling to discriminate between FCD subtypes and non-FCD epilepsy, such as generalised temporal lobe epilepsy (TLE), based on their epigenomic signature.[57] In another study, using gene set enrichment analysis (GSEA), Mills *et al.* found an increase in genes associated with the inflammatory response and an up-regulation of various microRNAs as well as a down-regulation of genes involved in neurite outgrowth and synaptic plasticity in TS lesions.[58]

Traditional descriptions of the pathology of FCD lesions have focussed on dysregulation in mTOR signalling and in particular of cells with abnormalities of cell size (DNs and BCs). But our study taken along with the increasing number of studies focussing on inflammation in FCD suggest that it is likely that complex cellular interactions between a range of cells play an important role in disease pathogenesis. This may be one of the reasons for the difficulty in treating the diseases by targeting just one molecule in a large functionally connected cellular and molecular network.[59]

IDENTIFYING CELLULAR SIGNALLING MOLECULES IN DEVELOPMENTAL DISORDERS OF THE BRAIN: EVIDENCE FROM FOCAL CORTICAL DYSPLASIA AND TUBEROUS SCLEROSIS

Neuropathology and
Applied Neurobiology—WILEY | 793
JOURNAL OF THE BRITISH NEUROPATHOLOGICAL SOCIETY

FIGURE 8 (A) Schematic diagram of the differences between the BCs and non-BCs (FCDIIA) groups according to the current literature. The difference between both groups is the presence of the balloon cells. In this proposed model, we suggest that there is more cellular heterogeneity in FCDIIB/TS and that the secretory factors CHI3L1 and CCL2 are produced by a population of small glia. (B) Our experiments indicate that these small glial and microglial cells reside close to BC's in FCDIIB and in cortical tubers from TS. We found that the expression of CHI3L1 and CCL2 diminished following inhibition of mTOR.
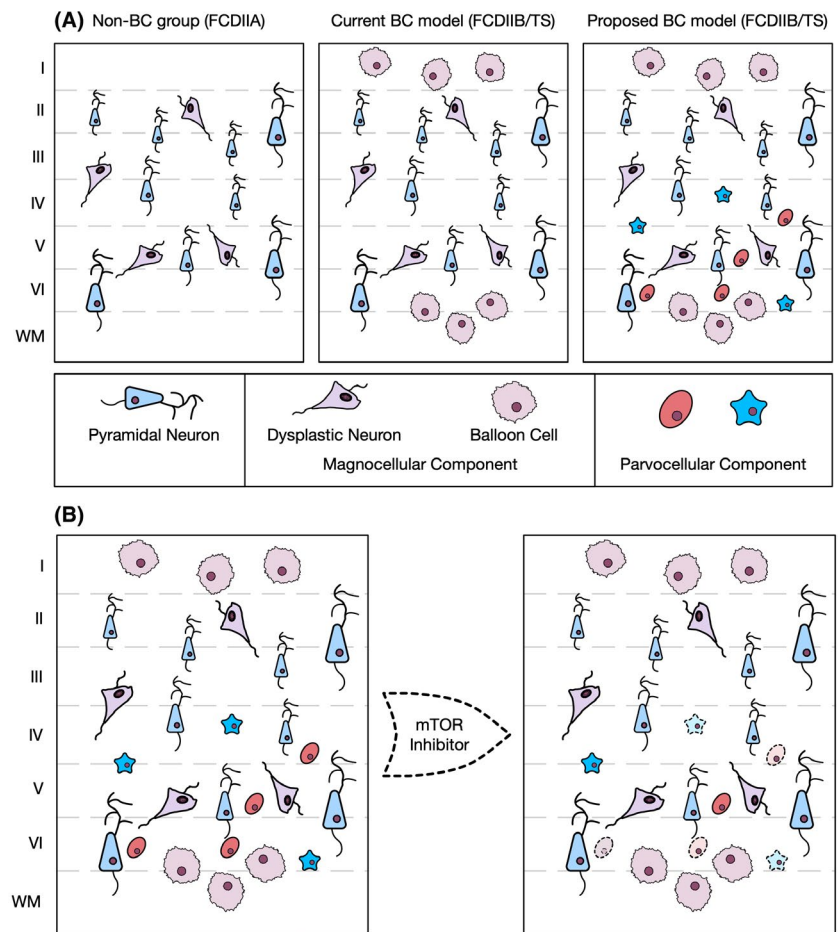
CONFLICT OF INTERESTS

The authors declare no conflict of interest. The Editors of Neuropathology and Applied Neurobiology are committed to peer-review integrity and upholding the highest standards of review. As such, this article was peer-reviewed by independent, anonymous expert referees and the authors (TSJ) had no role in either the editorial decision or the handling of the paper.

AUTHORS' CONTRIBUTIONS

YFL, FS, SRP, TJS, JCP, DAM, AA, AV, ARF, MT, WH, JHC, SAY, SMP and TSJ contributed to the collection and analysis of the data. DH, FG, SMP and TSJ led the design and conception of the study. YLF, TJS, SAY and TSJ wrote the manuscript.

ETHICAL STATEMENT

Ethical approval was obtained for this study. (REC Approval # 05/Q0508/129).

DATA SHARING

Most of the data is in the supplementary material. Additional data are available from the corresponding author.

PEER REVIEW

The peer review history for this article is available at https://publons.com/publon/10.1111/nan.12715.

ORCID

Jessica C. Pickles [iD] https://orcid.org/0000-0001-7888-1723
Thomas S. Jacques [iD] https://orcid.org/0000-0002-7833-2158

REFERENCES

1. Guerrini R, Dobyns WB. Malformations of cortical development: clinical features and genetic causes. *Lancet Neurol.* 2014;13:710-726.
2. Blumcke I, Spreafico R, Haaker G, et al. Histopathological findings in brain tissue obtained during epilepsy surgery. *N Engl J Med.* 2017;377:1648-1656.
3. Najm IM, Sarnat HB, Blumcke I. Review: the international consensus classification of focal cortical dysplasia – a critical update 2018. *Neuropathol Appl Neurobiol.* 2018;44:18-31.
4. Blümcke I, Thom M, Aronica E, et al. The clinicopathologic spectrum of focal cortical dysplasias: a consensus classification proposed by an ad hoc Task Force of the ILAE Diagnostic Methods Commission. *Epilepsia.* 2011;52:158-174.
5. Orlova KA, Crino PB. The tuberous sclerosis complex. *Ann N Y Acad Sci.* 2010;1184:87-105.

6. Crino PB, Nathanson KL, Henske EP. The tuberous sclerosis complex. *N Engl J Med*. 2006;355:1345-1356.

7. Becker AJ, Urbach H, Scheffler B, et al. Focal cortical dysplasia of Taylor's balloon cell type: mutational analysis of the TSC1 gene indicates a pathogenic relationship to tuberous sclerosis. *Ann Neurol*. 2002;52:29-37.

8. D'Gama AM, Woodworth MB, Hossain AA, et al. Somatic mutations activating the mTOR pathway in dorsal telencephalic progenitors cause a continuum of cortical dysplasias. *Cell Rep*. 2017;21:3754-3766.

9. Lim JS, Gopalappa R, Kim SH, et al. Somatic mutations in TSC1 and TSC2 cause focal cortical dysplasia. *Am J Hum Genet*. 2017;100:454-472.

10. Zimmer TS, Ciriminna G, Arena A, et al. Chronic activation of antioxidant pathways and iron accumulation in epileptogenic malformations. *Neuropathol Appl Neurobiol*. 2020;46(6):546-563.

11. Arena A, Zimmer TS, van Scheppingen J, et al. Oxidative stress and inflammation in a spectrum of epileptogenic cortical malformations: molecular insights into their interdependence. *Brain Pathol*. 2019;29:351-365.

12. Maroso M, Balosso S, Ravizza T, et al. Toll-like receptor 4 and high-mobility group box-1 are involved in ictogenesis and can be targeted to reduce seizures. *Nat Med*. 2010;16:413-419.

13. Picker S. Molecular Characterisation of Focal Cortical Dysplasia and Tuberous Sclerosis. Doctoral thesis, UCL (University College London) 2014.

14. Oliveira VC, Carrara RC, Simoes DL, et al. Sudan Black B treatment reduces autofluorescence and improves resolution of in situ hybridization specific fluorescent signals of brain sections. *Histol Histopathol*. 2010;25:1017-1024.

15. Stoppini L, Buchs PA, Muller D. A simple method for organotypic cultures of nervous tissue. *J Neurosci Methods*. 1991;37:173-182.

16. Daviaud N, Garbayo E, Schiller PC, Perez-Pinzon M, Montero-Menei CN. Organotypic cultures as tools for optimizing central nervous system cell therapies. *Exp Neurol*. 2013;248:429-440.

17. Humpel C. Organotypic brain slice cultures: a review. *Neuroscience*. 2015;305:86-98.

18. Grabiec U, Hohmann T, Hammer N, Dehghani F. Organotypic hippocampal slice cultures as a model to study neuroprotection and invasiveness of tumor cells. *J Vis Exp*. 2017;126:e55359.

19. Jensen SS, Petterson SA, Halle B, Aaberg-Jessen C, Kristensen BW. Effects of the lysosomal destabilizing drug siramesine on glioblastoma in vitro and in vivo. *BMC Cancer*. 2017;17:178.

20. Szabolcsi V, Celio MR. De novo expression of parvalbumin in ependymal cells in response to brain injury promotes ependymal remodeling and wound repair. *Glia*. 2015;63:567-594.

21. Weissinger F, Wawra M, Fidzinski P, et al. Dentate gyrus autonomous ictal activity in the status epilepticus rat model of epilepsy. *Brain Res*. 2017;1658:1-10.

22. Miller AP, Shah AS, Aperi BV, Kurpad SN, Stemper BD, Glavaski-Joksimovic A. Acute death of astrocytes in blast-exposed rat organotypic hippocampal slice cultures. *PLoS One*. 2017;12:e0173167.

23. Gritsenko P, Leenders W, Friedl P. Recapitulating in vivo-like plasticity of glioma cell invasion along blood vessels and in astrocyte-rich stroma. *Histochem Cell Biol*. 2017;148(4):395-406.

24. Kamikubo Y, Takasugi N, Niisato K, Hashimoto Y, Sakurai T. Consecutive analysis of BACE1 function on developing and developed neuronal cells. *J Alzheimers Dis*. 2017;56:641-653.

25. Chung K, Wallace J, Kim SY, et al. Structural and molecular interrogation of intact biological systems. *Nature*. 2013;497:332-337.

26. Liu AK, Hurry ME, Ng OT, et al. Bringing CLARITY to the human brain: visualization of Lewy pathology in three dimensions. *Neuropathol Appl Neurobiol*. 2016;42:573-587.

27. Liu Y, Namba T, Liu J, Suzuki R, Shioda S, Seki T. Glial fibrillary acidic protein-expressing neural progenitors give rise to immature neurons via early intermediate progenitors expressing both glial fibrillary acidic protein and neuronal markers in the adult hippocampus. *Neuroscience*. 2010;166:241-251.

28. Patro N, Naik A, Patro IK. Differential temporal expression of S100β in developing rat brain. *Frontiers in cellular neuroscience*. 2015;9:87.

29. Mamber C, Kamphuis W, Haring NL, Peprah N, Middeldorp J, Hol EM. GFAPδ expression in glia of the developmental and adolescent mouse brain. *PLoS One*. 2012;7:e52659.

30. Bonneh-Barkay D, Bissel SJ, Wang G, et al. YKL-40, a marker of simian immunodeficiency virus encephalitis, modulates the biological activity of basic fibroblast growth factor. *Am J Pathol*. 2008;173:130-143.

31. Llorens F, Thune K, Tahir W, et al. YKL-40 in the brain and cerebrospinal fluid of neurodegenerative dementias. *Mol Neurodegener*. 2017;12:83.

32. Querol-Vilaseca M, Colom-Cadena M, Pegueroles J, et al. YKL-40 (Chitinase 3-like I) is expressed in a subset of astrocytes in Alzheimer's disease and other tauopathies. *J Neuroinflammation*. 2017;14:118.

33. Sanfilippo C, Longo A, Lazzara F, et al. CHI3L1 and CHI3L2 overexpression in motor cortex and spinal cord of sALS patients. *Mol Cell Neurosci*. 2017;85:162-169.

34. Hinsinger G, Galeotti N, Nabholz N, et al. Chitinase 3-like proteins as diagnostic and prognostic biomarkers of multiple sclerosis. *Mult Scler J*. 2015;21:1251-1261.

35. Wiley CA, Bonneh-Barkay D, Dixon CE, et al. Role for mammalian chitinase 3-like protein 1 in traumatic brain injury. *Neuropathology*. 2015;35:95-106.

36. Brochner CB, Mollgard K. SSEA-4 and YKL-40 positive progenitor subtypes in the subventricular zone of developing human neocortex. *Glia*. 2016;64:90-104.

37. Qin G, Li X, Chen Z, et al. Prognostic value of YKL-40 in patients with glioblastoma: a systematic review and meta-analysis. *Mol Neurobiol*. 2017;54:3264-3270.

38. Bonneh-Barkay D, Bissel SJ, Kofler J, Starkey A, Wang G, Wiley CA. Astrocyte and macrophage regulation of YKL-40 expression and cellular response in neuroinflammation. *Brain Pathol*. 2012;22:530-546.

39. Bonneh-Barkay D, Wang G, Laframboise WA, Wiley CA, Bissel SJ. Exacerbation of experimental autoimmune encephalomyelitis in the absence of breast regression protein 39/chitinase 3-like 1. *J Neuropathol Exp Neurol*. 2012;71:948-958.

40. Junker N, Johansen JS, Hansen LT, Lund EL, Kristjansen PE. Regulation of YKL-40 expression during genotoxic or micro-environmental stress in human glioblastoma cells. *Cancer Sci*. 2005;96:183-190.

41. Boer K, Crino PB, Gorter JA, et al. Gene expression analysis of tuberous sclerosis complex cortical tubers reveals increased expression of adhesion and inflammatory factors. *Brain Pathol*. 2010;20:704-719.

42. Iyer A, Zurolo E, Spliet WG, et al. Evaluation of the innate and adaptive immunity in type I and type II focal cortical dysplasias. *Epilepsia*. 2010;51:1763-1773.

43. Broekaart DWM, Anink JJ, Baayen JC, et al. Activation of the innate immune system is evident throughout epileptogenesis and is associated with blood-brain barrier dysfunction and seizure progression. *Epilepsia*. 2018;59:1931-1944.

44. Mills JD, Iyer AM, Van Scheppingen J, et al. Coding and small non-coding transcriptional landscape of tuberous sclerosis complex cortical tubers: Implications for pathophysiology and treatment. *Sci Rep*. 2017;7:1-16.

45. Prabowo AS, Anink JJ, Lammens M, et al. Fetal brain lesions in tuberous sclerosis complex: TORC1 activation and inflammation. *Brain Pathol*. 2013;23:45-59.

46. Zhang Z, Liu Q, Liu M, et al. Upregulation of HMGB1-TLR4 inflammatory pathway in focal cortical dysplasia type II. *J Neuroinflammation*. 2018;15:27.

IDENTIFYING CELLULAR SIGNALLING MOLECULES IN DEVELOPMENTAL DISORDERS OF THE
BRAIN: EVIDENCE FROM FOCAL CORTICAL DYSPLASIA AND TUBEROUS SCLEROSIS

Neuropathology and
Applied Neurobiology—WILEY 795

47. Aronica E, Bauer S, Bozzi Y, et al. Neuroinflammatory targets and treatments for epilepsy validated in experimental models. *Epilepsia.* 2017;58:27-38.
48. Aronica E, Crino PB. Inflammation in epilepsy: clinical observations. *Epilepsia.* 2011;52:26-32.
49. Aronica E, Ravizza T, Zurolo E, Vezzani A. Astrocyte immune responses in epilepsy. *Glia.* 2012;60:1258-1268.
50. van Vliet EA, Aronica E, Vezzani A, Ravizza T. Review: neuroinflammatory pathways as treatment targets and biomarker candidates in epilepsy: emerging evidence from preclinical and clinical studies. *Neuropathol Appl Neurobiol.* 2018;44:91-111.
51. Vezzani A, French J, Bartfai T, Baram TZ. The role of inflammation in epilepsy. *Nat Rev Neurol.* 2011;7:31-40.
52. Mastellos DC. Complement emerges as a masterful regulator of CNS homeostasis, neural synaptic plasticity and cognitive function. *Exp Neurol.* 2014;261:469-474.
53. Perry VH, O'Connor V. C1q: The perfect complement for a synaptic feast? *Nat Rev Neurosci.* 2008;9:807-811.
54. Stephan AH, Barres BA, Stevens B. The complement system: an unexpected role in synaptic pruning during development and disease. *Annu Rev Neurosci.* 2012;369-389.
55. Stevens B, Allen NJ, Vazquez LE, et al. The classical complement cascade mediates CNS synapse elimination. *Cell.* 2007;131:1164-1178.
56. Aronica E, Crino PB. Epilepsy related to developmental tumors and malformations of cortical development. *Neurotherapeutics.* 2014;11:251-268.
57. Kobow K, Ziemann M, Kaipananickal H, et al. Genomic DNA methylation distinguishes subtypes of human focal cortical dysplasia. *Epilepsia.* 2019;60:1091-1103.
58. Mills JD, Iyer AM, van Scheppingen J, et al. Coding and small non-coding transcriptional landscape of tuberous sclerosis complex cortical tubers: implications for pathophysiology and treatment. *Sci Rep.* 2017;7:8089.
59. French JA, Lawson JA, Yapici Z, et al. Adjunctive everolimus therapy for treatment-resistant focal-onset seizures associated with tuberous sclerosis (EXIST-3): a phase 3, randomised, double-blind, placebo-controlled study. *Lancet.* 2016;388:2153-2163.

SUPPORTING INFORMATION

Additional supporting information may be found online in the Supporting Information section.